A&A 675, A199 (2023)
https://doi.org/10.1051/0004-6361/202346522

Astronomy & Astrophysics

XRBcats: Galactic low-mass X-ray binary catalogue*

A. Avakyan[1], M. Neumann[1], A. Zainab[2], V. Doroshenko[1], J. Wilms[2], and A. Santangelo[1]

[1] Universität Tübingen, Institut für Astronomie und Astrophysik Tübingen, Sand 1, 72076 Tübingen, Germany
e-mail: artur.avakyan@astro.uni-tuebingen.de

[2] Dr. Karl-Remeis Sternwarte and Erlangen Centre for Astroparticle Physics, Friedrich-Alexander Universität Erlangen-Nürnberg, Sternwartstr. 7, 96049 Bamberg, Germany

Received 28 March 2023 / Accepted 26 May 2023

ABSTRACT

We present a new catalogue of low-mass X-ray binaries (LMXBs) in the Galaxy. The catalogue contains source names, coordinates, source types, fluxes, distances, system parameters, and other characteristic properties of 349 LMXBs, including systems that have been newly discovered or reclassified since the most recently reported LMXB catalogues. The aim of this catalogue is to provide a list of all currently known Galactic objects identified as LMXBs with some basic information on each system (including X-ray and optical/IR properties where possible). Literature published before May 2023 has been taken into account where possible when compiling this information. References for all reported properties as well as object-finding charts in several energy bands are provided as part of the catalogue. We plan to update the catalogue regularly, in particular to reflect new objects discovered in the ongoing large-scale surveys such as *Gaia* and eROSITA.

Key words. catalogs – binaries: close – stars: late-type – X-rays: binaries

1. Introduction

X-ray binaries (XRBs) are among the brightest objects in the sky in the X-rays. They represent the endpoints of the stellar evolution of massive stars. Understanding the physical processes defining the observational appearance of individual objects and the properties of the XRB population as a whole is therefore essential for understanding massive star evolution and the evolution of the Galaxy in general. To this end, it is important to maintain an up-to-date census of known XRBs and their properties, especially in the era of the current generation of large-scale surveys such as the extended ROentgen Survey Imaging Telescope Array (eROSITA, Merloni et al. 2012; Predehl et al. 2021) on board SRG, *Gaia* (Gaia Collaboration 2016, 2023) and the Wide-field Infrared Survey Explorer (WISE, Wright et al. 2010; Cutri et al. 2021), which are able to unveil ever fainter objects.

However, the identification of XRBs among millions of other objects requires up-to-date knowledge of the properties and locations of already known sources, and the large-scale surveys mentioned above are providing vast amounts of new observational data for these objects. The compilation of such an updated database is the primary goal of this work, although many other uses can of course also be envisaged.

The main source of high-energy radiation in XRBs is the accretion of matter onto either a neutron star (NS) or a black hole (BH) from a companion star. The observed properties of XRBs are largely defined by the mass-transfer mechanism powering the accretion, which can occur either directly from the wind of a secondary or via Roche lobe overflow (RLOF), which primarily depends on the mass ratio between the compact object and the optical counterpart (M_x/M_{opt}). Based on this ratio, XRBs are subdivided into two large groups: high- and low-mass X-ray binaries (HMXBs and LMXBs, respectively). For objects with $M_x > M_{opt}; M_{opt} \lesssim 1\,M_\odot$, the mass is usually transferred to the compact object via RLOF. Such objects are classified as LMXBs. Those with $M_x < M_{opt}; M_{opt} \gtrsim 5\,M_\odot$ typically accrete directly from the stellar wind and are classified as HMXBs. The rather dramatic differences in the observed properties of LMXBs and HMXBs warrant the treatment of each subclass separately. Here, we focus on the properties of LMXBs. In turn, updated catalogues of HMXBs are presented by Neumann et al. (2023) and Fortin et al. (2023)[1,2].

As follows from the definition of an LMXB, the donor is (in most cases) a late-spectral-type star filling its Roche lobe. However, A-type stars, F-G-type subgiants, or even white dwarfs (WDs) can also act as donors in LMXBs. The optical properties of LMXBs can also be affected by emission from the accretion disc around the compact object, where the disc can be heated by itself or illuminated by X-ray emission from the compact object. Nevertheless, LMXBs are generally intrinsically faint objects in the optical and *IR* bands. The main way to analyse features of known LMXBs in detail or to detect new ones is to observe them during outbursts (Lasota 2016). New sources continue to be discovered in this way, and the population of known LMXBs is ever growing.

The latest catalogue of Galactic LMXBs, which was published by Liu et al. (2007), is now nearly 16 years old. Since that time, many new transient and persistent objects have been discovered. Some LMXB candidates have been reclassified, while

* The catalogue is available at the CDS via anonymous ftp to cdsarc.cds.unistra.fr (130.79.128.5) or via https://cdsarc.cds.unistra.fr/viz-bin/cat/J/A+A/675/A199, and the catalogue table, along with the corresponding finding charts and other useful information is also publicly accessible at http://astro.uni-tuebingen.de/~xrbcat

[1] https://vizier.cds.unistra.fr/viz-bin/VizieR?-source=J/A+A/671/A149

[2] https://binary-revolution.github.io/HMXBwebcat

other sources have gained LMXB status. Moreover, missions such as the X-ray Multi-Mirror Mission (*XMM-Newton*, Jansen et al. 2001), the INTErnational Gamma-Ray Astrophysics Laboratory (INTEGRAL, Winkler et al. 1993), and *Gaia* have resulted in a quantitative and qualitative improvement in our knowledge of XRB properties. In this context, we have compiled a revised catalogue of the Galactic LMXBs that incorporates multi-wavelength information and encompasses the inclusion of new sources identified since the publications of Liu et al. (2007) and Ritter & Kolb (2003; Liu07 and RK03 hereinafter). Our final catalogue contains 349 LMXBs and candidates, of which 204 were contained in the two catalogues mentioned above (the content of Liu07 and RK03 overlaps but neither includes the other completely). That is, the new catalogue presented here represents a more than 71% increase in volume with respect to the two most extensive catalogues of the past. We aim to compile a comprehensive and up-to-date database containing information such as optical/IR magnitudes, X-ray fluxes, distances, and so on, for the current catalogue, which will hopefully help to facilitate the identification of new LMXBs in current and future X-ray surveys, as well as population studies.

The structure of the paper is as follows: in Sect. 2, we describe how the LMXB sample was compiled and list data sources used to provide extra information on known objects. In the same section, we list relevant X-ray and optical properties, and characterise methods used for identification of known and candidate optical/IR counterparts in large-scale surveys. In Sect. 3, a description of the table fields and finding charts is provided, as well as a comparison of our catalogue with works of RK03 and Liu07. Finally, we summarise our results in Sect. 4. One can also find a list of identified archive optical/IR counterparts for some LMXBs based on the literature in Appendix A. A description of the columns of the catalogue table is presented in Appendix B.

2. Definition of the sample and data sources

The bulk of the objects in the catalogue consists of LMXBs reported by the catalogues of RK03 and Liu07, and so we started our compilation of the sample by merging these two catalogues. During this process, a number of duplicate objects both within and across the two catalogues were identified and removed from the sample. In addition, several sources in RK03 and Liu07 were found to be extragalactic (in some cases, this possibility was already indicated in the original catalogues and sometimes reported in the literature afterwards). Such objects were also excluded from our final list. The same applies to the satellite galaxies of the Milky Way. To this end, the two LMXBs known to be located in the Large Magellanic Cloud (LMC), namely, LMC X−2 and RX J0532.7−6926 (which were included in both RK03 and Liu07) are not listed in our catalogue. All objects that were removed, as well as other problematic cases, are listed and described in detail in Sect. 3.2.

In addition to Liu07 and RK03, we also considered all Galactic objects classified as possible LMXBs in the SIMBAD[3] and VizieR[4] databases hosted by the Centre de Données astronomiques de Strasbourg (CDS) databases. We include these objects in the catalogue, giving appropriate references for classification. We conducted a thorough literature search (including Astronomer's Telegrams[5]) to identify any newly discovered LMXBs. Most of the new LMXBs reported in the literature between 2006 and 2020 were discovered by the INTEGRAL (Winkler et al. 2003), MAXI (Matsuoka et al. 2009), *Swift* (Gehrels et al. 2004), or *Gaia* (Gaia Collaboration 2016) missions, as summarised by Bahramian & Degenaar (2023). The latter publication can therefore also be considered as another major data source used in this work. In addition, the catalogue of Galactic LMXBs detected by INTEGRAL (Sazonov et al. 2020) also proved to be a valuable resource for expanding our list of LMXBs. Finally, we used the recently published catalogue of ultracompact X-ray binaries (UCXBs) made by Armas Padilla et al. (2023)[6] to cross-check the completeness of our sample in the context of UCXBs (no missing sources were found). It should be noted that although efforts have been made to find all LMXBs identified to date, it is possible that some may have been missed. Therefore, we kindly ask readers to report any omissions found, so that those can be included in updated versions of the catalogue.

We note that systems in which a WD acts as an accretor are not generally considered as XRBs for historical reasons (despite the fact that they also emit in the X-ray band), and so those systems (namely cataclysmic variables or CVs) are not included in the current catalogue. We also do not include rotation-powered pulsars, even if they are members of binary systems and emit in X-rays, unless the observed emission is accretion powered; that is, 'spider'-type pulsars including Black Widows (BWs) and Redbacks (RBs; see e.g. Chen et al. 2013; Roberts 2013) are omitted unless they are also classified as transitional millisecond pulsars (tMSP; see e.g. Archibald et al. 2009; Papitto et al. 2013; Knight et al. 2023). All tMSPs and their candidates included in the catalogue are listed in Table 1 in Sect. 3.2.

The mass ranges quoted in Sect. 1 for XRBs are of course approximate, and there are some boundary cases, such as Her X−1, where accretion to a NS occurs via the RLOF of a B3 type ~2.2 $M_\odot$ donor (Tananbaum et al. 1972; Middleditch & Nelson 1976). This system is most often classified in the literature as an intermediate mass X-ray binary (IMXB) rather than as an LMXB because the NS appears as an X-ray pulsar and is therefore strongly magnetised, which is not typical for NS LMXBs. As the total number of IMXBs is relatively small, and despite the additional fact that they 'bridge' the HMXB and LMXB classes, they are evolutionarily closer to LMXBs as binary systems, and so we opt to include them as a part of the current LMXB catalogue. This decision is also clearly communicated in the publication describing the HMXB catalogue released in parallel to the current work (Neumann et al. 2023) in order to avoid any confusion or source duplication, except for one specific case (Cir X−1), which is described in Sect. 3.2.

2.1. Main properties and features

In order to reflect the huge variety of LMXB properties, we incorporate all accessible and relevant information concerning the donor star and compact object, including data on their properties, variability, and other pertinent details. Besides the quantitative properties (such as positions, fluxes in various bands, orbital or spin periods, and so on), some of these properties or features can be incorporated as a set of flags defined to characterise several LMXB subclasses, as was already done by Liu07 and RK03. Here, we extend the classification adopted by these authors to account for extra features added to the current catalogue. In order

[3] http://simbad.cds.unistra.fr/simbad
[4] https://vizier.cds.unistra.fr/viz-bin/VizieR
[5] https://astronomerstelegram.org
[6] https://research.iac.es/proyecto/compactos/UltraCompCAT

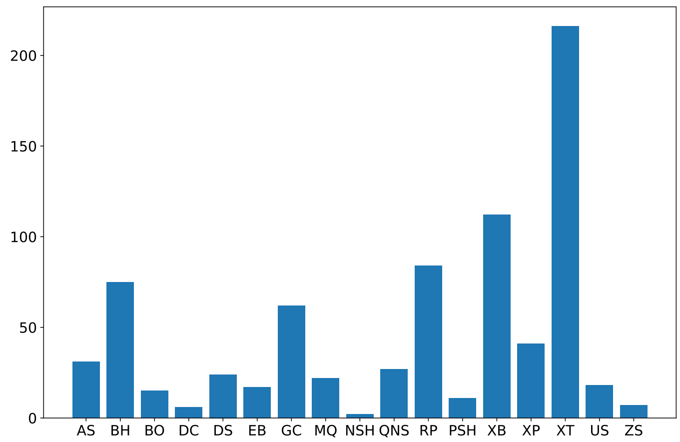

Fig. 1. Population of LMXBs of each type in the Galaxy.

to provide a broad overview of the Galactic LMXB properties, we also show the frequency of the occurrence of the individual type flags in graphical format in Fig. 1. It is important to note that these flags are not intended to serve as a basis for systematic classification, but rather to reflect the characteristics of individual systems to ease the selection of objects exhibiting specific observational features. Each source in the catalogue may therefore have one or more of the following flags, which are listed alphabetically:

1. AS: Atoll X-ray binary hosting a weakly magnetised NS as a main component. The spectrum is soft and no significant pulsations are present. The majority of the points on the colour–colour diagrams ('hard' versus 'soft') from atoll sources usually form a band at constant hard colour.
2. BH: System contains a black hole candidate.
3. BO: X-ray burster (see XB definition below) with coherent burst oscillations at the NS spin period.
4. DC: System with an accretion disc corona.
5. DS: 'Dipping' source. System shows periodic but irregular dips in the X-ray intensity, which are generally connected with the partial obscuration of the NS by a thickened region of the accretion disc.
6. EB: Eclipsing or partially eclipsing binary system.
7. GC: Source within a globular cluster.
8. MQ: Microquasar, a source with reported evidence for relativistic jets.
9. NSH: Negative (nodal) superhumps are present in the system. These negative superhumps are periodic optical signals, the periods of which are smaller than the orbital period of the binary.
10. QNS: Quiescent NS.
11. RP: Compact object acts as a radio pulsar.
12. PSH: Positive superhumps (permanent or transient) present in the system. The same as the NSH type (see above), but the time period of the signal is larger than the orbital one.
13. XB: X-ray burst source. This type collects X-ray binary systems with a NS, which exhibit thermonuclear (type-I) X-ray bursts.
14. XP: Compact object in the binary acts as an X-ray pulsar.
15. XT: Transient X-ray source. System shows dramatic changes in luminosity (mostly in the X-ray band). Energy is produced by means of a non-stationary accretion process.
16. US: Ultrasoft X-ray spectrum. In some catalogues, this type is denoted 'super soft'. These binaries also include some 'extreme ultrasoft' (EUS) sources.
17. ZS: Z-type source. This type of X-ray binary is similar to the atoll type (also contains weakly magnetised NS), but the plot on the colour–colour diagram is different (Z-letter shape).

We note that the 'XB' (X-ray burster) flag – originally introduced by RK03 – in our catalogue specifically refers to thermonuclear (type-I) bursts only. Type-II X-ray bursts likely caused by instabilities in the accretion flow are relatively rare, and to the best of our knowledge have only been detected from two LMXBs: MXB 1730−335 ('rapid burster'; Bagnoli et al. 2015) and GRO J1744−28 ('bursting pulsar'; Court et al. 2018), and one HMXB: SMC X−1 (Rai et al. 2018), and are therefore not flagged separately. The MXB 1730−335 is known to exhibit bursts of both types, and is therefore still flagged. On the other hand, type-I bursts have been suggested to be present but have never been unambiguously detected from the bursting pulsar (Giles et al. 1996; Lamb et al. 1996; Doroshenko et al. 2015), and so this source is not flagged.

2.2. X-ray properties

Considering that X-ray emission dominates the bolometric luminosity of XRBs, one of their main characteristics is their X-ray flux and spectrum. In our catalogue, we therefore tried to compile information on X-ray fluxes in soft and hard X-ray bands for all LMXBs in a uniform way. For the soft X-ray band, we report fluxes observed by *XMM-Newton*[7] (Schartel et al. 2022; Webb et al. 2020), the *Chandra* X-ray Observatory[8] (CXO, Weisskopf et al. 2000; Evans et al. 2010), and *Swift*/XRT[9] (Burrows et al. 2005; Evans et al. 2020) throughout their lifetime. In particular, we report the 0.2–12 keV energy band flux (equivalent to the EPIC_8 band used in *XMM-Newton* catalogues) and/or the X-ray flux in similar energy bands of CXO and *Swift*/XRT, that is, the 0.3–10 keV observed flux for *Swift*/XRT, and either the broad ACIS band (0.5–7.0 keV) or the wide HRC band (0.1–10.0 keV) for CXO. We note that although the difference in energy bands for various instruments might result in a factor of ~1.5 difference for a given source, here we only report the range of fluxes detected over a long period. This range is therefore dominated by intrinsic variability and differences in source spectra, and so the difference in energy range between the various instruments is not really relevant to our purposes. In the hard X-ray band, fluxes from INTEGRAL[10] (Krivonos et al. 2012) and *Swift*/BAT[11] (Oh et al. 2018; Barthelmy 2004) are reported. Here, we report fluxes in the energy range of 14–145 keV for *Swift*/BAT and in the energy range of 17–60 keV for INTEGRAL. We note that these bands are largely equivalent as the flux above 60 keV is comparatively small for most sources, and the variability argument still applies.

Another key property provided by X-ray observations is the localisation that is essential to identify or assess the reliability of the identified optical counterparts. We therefore also include information on the most accurate X-ray position available either from the literature or directly from soft (*Chandra*, *XMM-Newton*

[7] https://heasarc.gsfc.nasa.gov/W3Browse/xmm-newton/xmmssc.html
[8] https://vizier.cds.unistra.fr/viz-bin/VizieR-3?-source=IX/57/csc2master
[9] https://vizier.cds.unistra.fr/viz-bin/VizieR-3?-source=IX/58/2sxps
[10] https://vizier.cds.unistra.fr/viz-bin/VizieR-3?-source=J/A%2bA/545/A27
[11] https://heasarc.gsfc.nasa.gov/W3Browse/swift/swbat105m.html

or *Swift*/XRT) and hard (INTEGRAL, *Swift*/BAT) catalogues as described in the following section.

2.3. Astrometry and identification of the optical counterparts

Considering that the properties of XRBs are largely defined by the properties of the donor star, the identification of the optical counterparts and the characterisation of their multi-wavelength properties are essential. Some of the LMXBs in the sample already have robustly identified optical counterparts; however, the optical positions (as well as other optical data) reported in Liu07 and RK03 are in many cases outdated, and lack accuracy by current standards. We therefore attempted to improve position accuracy using the latest astrometry data from *Gaia* DR2[12], eDR3[13], DR3[14] (Gaia Collaboration 2018, 2021, 2023), Two Micron All Sky Survey[15] (2MASS, Skrutskie et al. 2006; Cutri et al. 2003b,a) and the mid-IR CatWISE2020 catalogue[16] (Marocco et al. 2021).

We started the process of identifying counterparts in these catalogues by verifying whether the SIMBAD database already had any pre-existing matches with *Gaia* DR3 (eDR3, DR2), 2MASS, and/or WISE and checking their correctness manually. It should be noted that in some cases, the associations provided by SIMBAD were indeed incorrect, and we list such cases in Sect. 3.2. In cases where no SIMBAD optical/IR identifiers were provided, we attempted to find counterparts reported in the literature. In some cases where precise optical, IR, or radio coordinates were available, these coordinates were used to find the corresponding counterparts in *Gaia* DR3, 2MASS, and CatWISE2020. All solid cross-matches and relevant data were added to the catalogue. In particular, identifications by Arnason et al. (2021) proved to be useful, and so these are considered as the main references for the cases marked in Table A.1. This table lists all sources for which optical/IR counterparts are available, except those correctly listed in SIMBAD.

As mentioned above, some LMXBs have been classified as such only based on their X-ray properties, and have no uniquely identified optical counterparts in the literature. In most cases, these are relatively poorly studied sources (sometimes only detected once with X-ray monitors during an outburst). However, in some cases, accurate X-ray positions obtained at a later time are available. For those objects, we used CXO, *XMM-Newton*, or *Swift*/XRT positions (in order of preference). The search radius was set to match the full positional uncertainty (i.e. statistical plus systematic) reported in the respective X-ray catalogue. The final identification of plausible optical counterparts was done manually by inspection of the finding charts also released as part of the current catalogues and by searching for tentative counterparts in the literature based on their properties. In all cases where it was possible to identify a plausible counterpart, we list it as such; however, the optical position is only assigned as primary if a unique counterpart is identified.

2.4. Additional information

For all optical counterparts identified as described above, we include information on IR and/or optical magnitudes wherever possible. In particular, we include *Gaia* G-band or V-band magnitudes in the optical band, near-IR photometry either from 2MASS or Visible and Infrared Survey Telescope for Astronomy (VISTA, Emerson et al. 2006; Dalton et al. 2006) Variables in the Via Lactea (VVV) DR4 catalogue (VVV[17], Minniti et al. 2010) surveys, or from the literature. Finally, we also include magnitudes in the $W1$ and $W2$ bands reported in the CatWISE2020, AllWISE, or WISE (in that order of preference) catalogues (Marocco et al. 2021; Cutri et al. 2021; Wright et al. 2010). In all cases, we provide the references to the sources where the V-band, G-band, JHK, and WISE magnitudes were taken from and show them in 'Vmag_Ref', 'Gmag_Ref', 'JHK_Ref', and 'WISE_Ref' columns, respectively. It should be noted that we mainly tried to include the optical/IR magnitudes during the quiescent state of the corresponding binary (to represent the LMXB population in the state in which it is found most of the time). However, in some cases, 'quiescent' magnitudes were not available, and so we list magnitudes during the outburst, if any.

Besides more accurate positions and photometry, we also include some additional information unavailable at the time of publication of Liu07 and RK03. For all LMXBs for which a *Gaia* counterpart was ultimately identified, we provide distance estimates from *Gaia* DR3, those based on *Gaia* eDR3[18] (Bailer-Jones et al. 2021) or *Gaia* DR2[19] (Bailer-Jones et al. 2018), and estimations from StarHorse1[20]/2[21] (Anders et al. 2019, 2022). In addition, we manually searched the literature for any distance estimations, especially in cases where *Gaia*/StarHorse data were unavailable.

We were also interested in the spectral type of the optical counterpart, and we therefore attempted to include this information based on either *Gaia* DR3, SIMBAD, or the literature search. We note that the list of X-ray pulsars maintained by Mauro Orlandini[22] was found to be a useful resource in this regard (and also for reported spin and orbital periods) and we would like to acknowledge it here. For sources where the reported spectral type and corresponding reference were published before 2007, the spectral information in RK03 or Liu07 was used.

Finally, for convenience, we also provide the X-ray absorption neutral hydrogen column density ($N_{\rm H}$) estimates, which might be relevant to estimate some additional LXMB properties such as X-ray to optical luminosity ratios in order to facilitate searches for new LMXBs with similar properties. We report values based either on *Swift*/XRT data (Evans et al. 2020) or on results reported in the literature (all references are listed). In cases where one of the two ($N_{\rm H}$ or $A_{\rm G}$) was unknown, we calculated the other one through the $N_{\rm H}(A_{\rm G})$ relation reported by Foight et al. (2016).

[12] https://vizier.cds.unistra.fr/viz-bin/VizieR?-source=I/345
[13] https://vizier.cds.unistra.fr/viz-bin/VizieR-3?-source=I/350/gaiaedr3
[14] https://vizier.cds.unistra.fr/viz-bin/VizieR-3?-source=I/355
[15] https://vizier.cds.unistra.fr/viz-bin/VizieR?-source=II/246
[16] https://vizier.cds.unistra.fr/viz-bin/VizieR?-source=II/365
[17] http://vvvsurvey.org
[18] https://vizier.cds.unistra.fr/viz-bin/VizieR-3?-source=I/352
[19] https://vizier.cds.unistra.fr/viz-bin/VizieR-3?-source=I/347
[20] https://vizier.cds.unistra.fr/viz-bin/VizieR-3?-source=I/349/starhorse
[21] https://vizier.cds.unistra.fr/viz-bin/VizieR-3?-source=I/354/starhorse2021
[22] http://www.iasfbo.inaf.it/~mauro/pulsar_list.html

3. Catalogue content and quality assurance

3.1. Description of the fields

There are 349 entries in the catalogue, each of which corresponds to a single Galactic source. The objects are sorted by right ascension (the second column) in increasing order. There are a total of 62 columns listing various parameters and corresponding references. The content and format of individual columns is described in detail in Table B.1.

3.2. Finding charts and problematic cases

We provide finding charts for all sources in our catalogue, which includes up to six different images, covering bands from mid-IR to hard X-rays. Corresponding charts can be found on a dedicated website[23] or obtained via CDS system[24]. The top row of each finding chart includes images from the VVV DR4 catalogue[25] (Minniti et al. 2010) or 2MASS[26] (left, in order of preference), an image of unWISE[27] (Schlafly et al. 2019; middle), and an RGB-image of either *Chandra*[28], *XMM-Newton*[29], or the Roentgensatellit (ROSAT[30], Truemper 1982; Boller et al. 2016; Voges et al. 1999; right, in order of preference).

The bottom row includes the soft X-ray image of *Swift*/XRT (SwiftXRTInt in astroquery.skyview) in the left corner, and hard X-ray images from *Swift*/BAT[31] and INTEGRAL[32] in the middle and right corners, respectively. The field of view for *VVV*, 2MASS, unWISE, *XMM-Newton*, and *Chandra* images was set at 1 arcmin, while for *Swift*/XRT and ROSAT it was set at 5 arcmin and 15 arcmin, respectively. The field of view for *Swift*/BAT and INTEGRAL was chosen to be 10°, with the size of the region chosen based on the field of view and angular resolution of the given instrument.

Each panel of the finding chart includes the coordinates and uncertainties of all detected sources within the respective regions, with position uncertainties represented by error circles. A red cross indicates the position listed in SIMBAD for the source, while a dark-blue diamond represents the coordinates described in the literature (Liu07 or RK03). The position used for this catalogue is indicated with an orange star. In the case of soft X-ray instruments, observation positions are indicated by error circles to prevent overcrowding. A golden circle indicates the *Chandra* position, a red circle indicates the *XMM-Newton* position, a green circle indicates the *Swift*/XRT position, and a navy-blue circle indicates the ROSAT position. *Swift*/BAT and INTEGRAL are indicated as a deep-pink pentagon and a lime-green triangle, respectively. In the optical band, we indicate CatWISE2020 with an orange 'X', 2MASS with a cyan '+', and *Gaia* DR3 data with a purple square. From a technical perspective, we used the Hierarchical Progressive Surveys (HiPS) data from Fernique et al. 2015, using SkyView Query only for *Swift*/XRT to obtain images. Both services were queried using `astroquery.hips2fits`[33], and `astroquery.skyview`[34] modules.

As an example, the finding chart of GRO J1744−28 can be seen in Fig. 2. We also note that imaging in more bands with a catalogue overlay is available via the Aladin lite interface (Baumann et al. 2022) on the website hosting the catalogue[35].

Based on the literature search and inspection of the finding charts described above, we identified several problematic cases:

- The X-ray source SAX J0840.7+2248, which is classified as a LMXB in Liu07, is excluded from our catalogue. This transient is more likely to be the X-ray-rich gamma-ray burst GRB980429 rather than an XRB (Sidoli et al. 2007).
- J0732.6−1330, which is listed as a LMXB in SIMBAD, is also not presented in our catalogue due to the fact that the source is an intermediate polar (accreting magnetised white dwarf, IP; Butters et al. 2007).
- Peng & Shen (2021) find the LMXB candidate OGLE BLG511.6 25872 to be of the same polar nature. We therefore do not include it in our catalogue.
- The X-ray transient Swift J061223.0+701243(.9), listed as LMXB in Liu07, could also be an IP (Butters et al. 2011). In this case, the authors suggest that an LMXB nature cannot be ruled out, and so the source can still be found in our catalogue; however, we urge caution when considering the classification of this source.
- 2E 1613.5−5053 (listed as 1E 161348−5055.1 in Liu07 LMXB catalogue) is an X-ray source located close to the centre of the supernova remnant RCW 103. Based on XMM observations, it was discovered that the source has a 6.67 h periodicity, which may originate from either an orbital period of a LMXB or a spin period of an isolated neutron star (INS; De Luca et al. 2006). After some time of searching for an optical/IR counterpart to confirm or refute a binary nature origin, Tendulkar et al. (2017) finally reported the detection of an IR counterpart, the properties of which clearly indicate that the IR emission was coming from an INS, ruling out an LMXB origin scenario.
- V* V934 Cen, another SIMBAD LMXB, seems to possess no XRB characteristics (the corresponding link in SIMBAD for the suggested LMXB type does not provide any data regarding the source), and so it is excluded from our catalogue as well.
- The same also goes for the binary TWA 22 (TWA 22AB), which is considered to be a LMXB in the SIMBAD database. SIMBAD refers to Bonnefoy et al. (2009) as the source of the corresponding classification. However, these authors estimated the total mass of the binary to be about a 220 $M_{\rm Jup}$, which is far too low for the XRB. Although the system emits X-rays via coronal activity (Stelzer et al. 2022), it cannot be classified as an XRB.
- 4U 1745−203 (H 1745−203) is a transient that was considered to be a separate LMXB, but the source appears to simply be a counterpart of SAX J1748.9−2021 (NGC 6440 CX1), which has already been noted in Liu07.
- The same goes for bursting source MXB 1742−29. Following Martí et al. (2007), we consider it to be the counterpart of LMXB 1A 1742−294.

[23] http://astro.uni-tuebingen.de/~xrbcat
[24] https://cdsarc.cds.unistra.fr/cgi-bin/qcat?J/A+A
[25] http://alasky.cds.unistra.fr/VISTA/VVV_DR4/VISTA-VVV-DR4-J
[26] http://alasky.cds.unistra.fr/2MASS/J
[27] http://alasky.cds.unistra.fr/unWISE/W1
[28] https://cdaftp.cfa.harvard.edu/cxc-hips
[29] http://skies.esac.esa.int/XMM-Newton/EPIC-RGB
[30] http://alasky.cds.unistra.fr/RASS
[31] http://cade.irap.omp.eu/documents/Ancillary/4Aladin/BAT_14_20
[32] http://cade.irap.omp.eu/documents/Ancillary/4Aladin/INTEGRAL_17_60
[33] https://astroquery.readthedocs.io/en/latest/hips2fits/hips2fits.html
[34] https://astroquery.readthedocs.io/en/latest/skyview/skyview.html
[35] http://astro.uni-tuebingen.de/~xrbcat

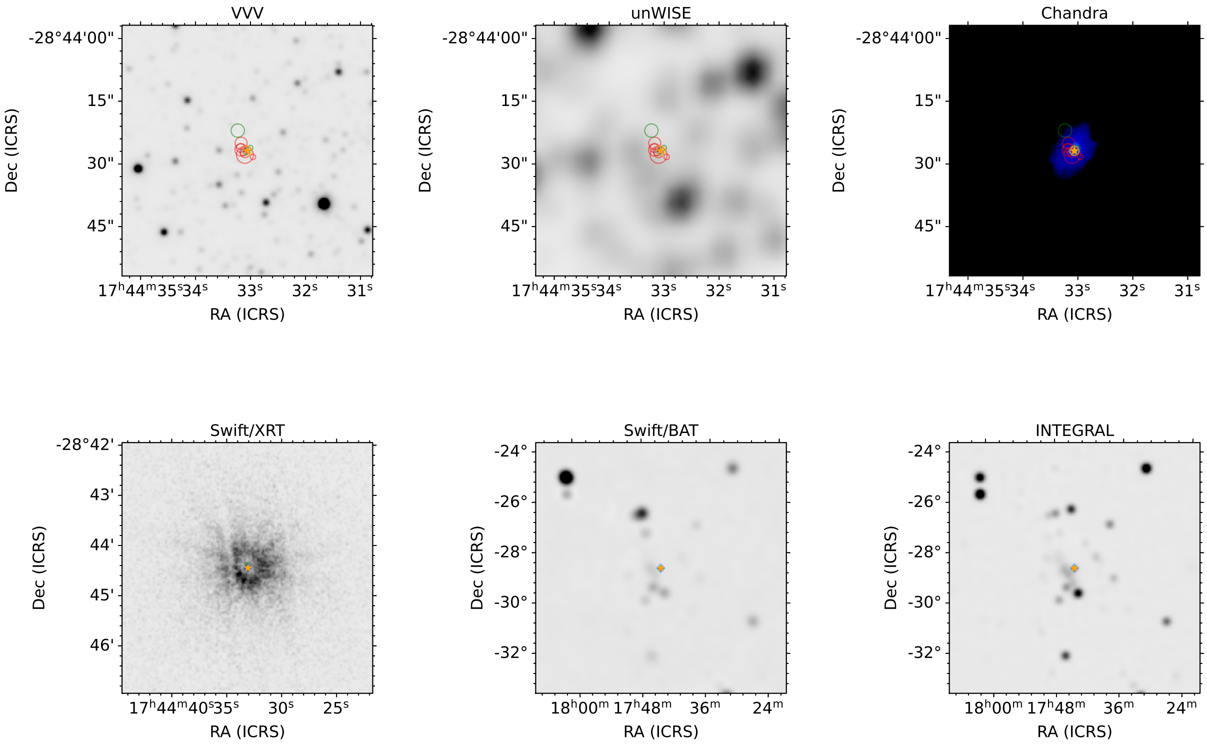

Fig. 2. Finding chart of GRO J1744−28. The finding charts display markers and error circles representing observations made by different instruments. The error circles are used for soft X-ray observations to prevent overcrowding, with a yellow circle indicating *Chandra* and a green circle representing *Swift*/XRT. The red cross and the blue diamond indicate the positions reported by SIMBAD and that found in the literature (Liu07 or RK03), respectively. An orange star denotes the position of the LMXB used in this catalogue.

- AX J1620.1−5002 is also an X-ray transient, which for a long time was considered to be a separate XRB, but it is now strongly associated with the bursting transient LMXB MAXI J1621−501 (Chenevez et al. 2018; Gorgone et al. 2018).
- 4U 0614+09 (4U 0614+091) is an UCXB with an uncertain orbital period, which is only constrained to be greater than 1 h (Baglio et al. 2014). However, following Liu07 and RK03 in the catalogue, we provide a value of 51.3 min based on Shahbaz et al. (2008).
- The nature of IGR J17404−3655 is not well constrained, because it is unclear whether the source is a LMXB or a HMXB, and is potentially a BeXRB (Coleiro et al. 2013). However, Fortin et al. (2018) used *K*-band spectroscopy for the source, and revealed that the object is more likely to be a CV with a K3–5V donor star. Consequently, we made the decision to not include it.
- CXOGBS J174623.5−310550 is an accreting binary, and is presented in our catalogue. However, its exact classification, that is, as either LMXB or CV, is still unknown (Torres et al. 2019).
- 1RXS J180431.1−273932 was at first considered a symbiotic LMXB system (Nucita et al. 2007) hosting a NS with a M5 III donor star. However, based on optical observations, Masetti et al. (2012) excluded a possible symbiotic LMXB nature and identified the source as a magnetic CV. Therefore, despite the fact that 1RXS J180431.1−273932 is listed as a symbiotic X-ray binary in Kuranov & Postnov (2015), we do not include it.
- Based on IR observations of 4U 1556−60 made by Revnivtsev et al. (2013), we associated an optical counterpart to this source, namely *Gaia* DR3 5833042299288809907 (see Table A.1), which lies well inside the position error circle of $0\farcs3$. However, according to the provided parallax, the distance to this source should not exceed 1kpc (Bailer-Jones et al. 2021), which is 3–4 times less than the distance estimations to 4U 1556−60 (Christian & Swank 1997; Grimm et al. 2002). We decided to leave this association with the *Gaia* DR3 source, but this discrepancy should be borne in mind.
- For the source IGR J17597−2201, Walter et al. (2006) proposed 2MASS J17594556−2201435 as a potential counterpart. However, based on Very Large Telescope (VLT) observations conducted by Fortin et al. (2018), we can exclude this possibility.
- The persistent X-ray-bright LMXB 4U 1624−49 seems to have incorrect coordinates and optical/IR associations in the SIMBAD database. The source was localised by *Chandra* with $0\farcs6$ uncertainty at the position $\alpha_{J2000.0} = 16^h28^m02\fs825$, $\delta_{J2000.0} = -49°11'54\farcs61$ (Wachter et al. 2005), which corresponds to the known XMM source 2XMM J162802.8−491154, which is located ≈ 53″ away from the position of 4U 1624−49 in SIMBAD. In our table, we provide the *Chandra* coordinates and uncertainty, as well as the *K*-band data obtained by Wachter et al. (2005). In the corresponding *Chandra* error circle, there are no *Gaia*, 2MASS, or CatWISE2020 sources. We also label 2XMM J162802.8−491154 as an alternative name for 4U 1624−49 due to the fact that this name is not listed as an identifier for this source in any other databases to the best of our knowledge.
- There is also an incorrect SIMBAD association with optical/IR archives for the LMXB GX 5−1 (4U 1758−25). At the position provided by SIMBAD, there is a bright star

located ≈ 200 pc away (Gaia Collaboration 2023), a distance which is totally inconsistent with distance estimations for GX 5−1 (4.2–5.6 kpc, according to Clark 2018). Jonker et al. (2000) found an IR counterpart of the X-ray source at the position $\alpha_{J2000.0} = 18^{h}01^{m}08\overset{s}{.}222$, $\delta_{J2000.0} = -25°04'42\overset{''}{.}46$ with $0\overset{''}{.}35$ uncertainty, leading to it being located ≈ 20″ away from the position of GX 5−1 in SIMBAD. As in the case of 4U 1624–49, there are no *Gaia*, 2MASS, or CatWISE2020 counterparts. However, in the error circle, we find a VVV source, for which the JHK magnitudes are provided in the table.

– We also decided to add the object named AX J1659.0−4208 as a LMXB in our catalogue. The source was detected during the Advanced Satellite for Cosmology and Astrophysics (ASCA) Galactic plane survey (Sugizaki et al. 2001). At the time, the X-ray flux of the source was at the level of 6×10^{-12} erg s^{-1} cm^{-2} (0.7–10 keV), but its coordinates were not well constrained. Its accurate position was then derived by *Chandra*, which led to identification of a near-IR counterpart by Revnivtsev et al. (2013). These latter authors suggested that the source is likely to be a symbiotic LMXB or a CV. However, based on high extinction towards this area, and distance estimations of about 5–10 kpc (Revnivtsev et al. 2013), unabsorbed X-ray luminosity can be estimated to be 10^{34} erg s^{-1} at the very least (most likely even 10^{35} erg s^{-1}), which is significantly greater than expected for a typical CV. We therefore suggest that the source is very likely to be a LMXB and it is added to our catalogue table.
– We add an X-ray source IGR J19308+0530, which seems to be an IMXB hosting an NS and s F4V-type donor star (Fortin et al. 2018). At first it was not clear whether the object is a CV or a L/IMXB (Ratti et al. 2013), and even the SIMBAD database presents the source as a CV. However, based on the spectral analysis (Ratti et al. 2010) and *K*-band spectroscopy (Fortin et al. 2018), we suggest that IGR J19308+0530 is most likely not a CV but an IMXB. It should also be noted that the star TYC 486−295−1 is a counterpart of IGR J19308+0530 (Rodriguez et al. 2008; Ratti et al. 2010), but it is considered to be a separate source (also a CV type instead of XRB) by SIMBAD, ≈88″ away from the INTEGRAL position for IGR J19308+0530 listed in SIMBAD.
– The source LMXB 4U 1728−34 was given an orbital period of ∼11 min (Galloway et al. 2010), and this value is also given for the binary in RK03. However, in an analysis of other X-ray observations, no further evidence was found for a periodic signal at 11 min. Subsequently, based on an analysis of its type-I X-ray burst, Vincentelli et al. (2020) stated that the orbital period should be much higher, probably ∼66 min or even ≳2 h. In our catalogue, the value of 66 min is quoted, but readers should be aware of the lack of robust confirmation.
– The X-ray source J2039−5617 (listed as [SMD2015] 3 in SIMBAD) is presented in the RK03 catalogue as a LMXB. However, due to a likely association with the known RB source 1FGL J2039.4−5621 (Salvetti et al. 2015), it is excluded from our catalogue.
– XB 1832−330 is a globular cluster LMXB (in NGC 6652) that was tentatively assigned a 43.6 min orbital period (Deutsch et al. 2000). However, Engel et al. (2012) argue that the 43.6 min candidate period is probably spurious and suggest a longer period (by a factor 3) of about 2.15 h (this value is quoted in our catalogue).

Table 1. tMSP candidates presented in our catalogue.

Source name	References
1FGL J1417.7−4407 (J1417−4402 in RK03)	[1]
CXOGlb J183544.5−325939 (NGC 6652B)	[2]
4FGL J0427.8−6704	[3], [4]
4FGL J0407.7−5702	[5]
CXOGlb J174804.5−244641 (Terzan 5 CX1)	[6]
CXOU J110926.4−650224	[7], [8]
3FGL J1544.6−1125	[9], [10], [11]
4FGL J0540.0−7552	[12]
RX J1739.4−2942 (GRS 1736−297)	[13]

Notes. Along with the candidates, all three confirmed tMSPs: XSS J12270−4859, IGR J18245−2452 and PSR J1023+0038 are also included in the catalogue.
References. [1] Swihart et al. (2018), [2] Paduano et al. (2021), [3] Kennedy et al. (2020), [4] Li et al. (2020), [5] Miller et al. (2020), [6] Bahramian et al. (2018), [7] Coti Zelati et al. (2019), [8] Coti Zelati et al. (2021), [9] Bogdanov & Halpern (2015), [10] Britt et al. (2017), [11] Jaodand et al. (2021), [12] Strader et al. (2021), [13] Tetarenko et al. (2016).

– There is uncertainty over the orbital period of the tMSP candidate 4FGL J0540.0−7552. Strader et al. (2021) identified a consistent periodic signal at 2.7 h in their photometry. However, this signal could represent either the orbital period, half the orbital period (if due to ellipsoidal variations), or could even be spurious. We decided to keep the 2.7 h orbital period value in our catalogue table for this source, but other possibilities may be worth consideration.

As mentioned in Sect. 1, we decided to add all three known tMSP: XSS J12270−4859, IGR J18245−2452, and PSR J1023+0038 (all three are also listed in RK03 by the names J1227−4853, J1824−2452, and AY Sex, respectively). In addition, we include some tMSP candidates identified as such in the literature, which can be found in Table 1 with references. In the catalogue table itself, one can find a corresponding flag column named 'tMSP_Flag' (see Table B.1).

Several objects originally listed in the HMXB catalogue of Liu et al. (2006) are now moved to the current LMXB catalogue as their preferred classification changed:
– According to Karasev et al. (2008), XTE J1901+014 was suggested to be the first low-mass fast X-ray transient. However, the exact nature of this source remains unclear. Nevertheless, according to Sato et al. (2019), it appears to be more similar to a LMXB, hence its inclusion in our catalogue.
– IGR J16358−4726 was initially identified as an HMXB by Chaty et al. (2008). However, Nespoli et al. (2010) later invalidated this identification, and now the source is classified as a symbiotic X-ray binary, which we consider to be a LMXB subclass based on the typical donor mass.
– The situation is similar for IGR J17407−2808. This source was first classified as part of a supergiant fast X-ray transients (SFXT, Sguera et al. 2006), which are all HMXBs. However, subsequent works (Heinke et al. 2009; Greiss et al. 2011) ruled out the presence of a supergiant companion, and showed that this source is more likely to be a LMXB with an F-type dwarf. Kaur et al. (2011) also found that a few days after the outburst, the IR counterpart was 1 mag brighter. Such behaviour is more expected during the LMXB outburst due to the exposure of the optical component to the X-rays emitted by the compact object.

- After analysing the X-ray spectra and near-IR observations of SAX J1452.8−5949, Kaur et al. (2009) were able to estimate the distance to SAX J1452.8−5949 ($\lesssim$10 kpc). This estimation eliminated the possibility of the system being a HMXB, as it would have to be an extragalactic source in that case. Consequently, the authors suggested that the binary has a low-mass companion and could either be a LMXB or an IP. Therefore, we classify SAX J1452.8−5949 as a LMXB candidate.
- It has been unclear for some time whether 4U 1807−10 is a HMXB or a LMXB. However, based on the ratio of spin and orbital periods (Blay et al. 2008), as well as the fact that the system shows type-I X-ray bursts (Chelovekov et al. 2017), we conclude that an LMXB origin is more likely for this source, despite the fact that 4U 1807−10 is marked as a HMXB candidate in Blay et al. (2008), and therefore we add 4U 1807−10 to our LMXB catalogue.

In addition, there is one source that is present in both of our catalogues, in this one, and in the one dedicated to HMXBs (Neumann et al. 2023). This is due to the presence of conflicting results and the absence of any final decision on the true nature of the source:

- Cir X−1 was originally classified as a LMXB after its discovery. However, Heinz et al. (2013) were able to determine that the system is only about 4500 yr old, which led to a revision of its classification. Additionally, Jonker et al. (2007) reported that Cir X−1 contains a supergiant companion of A0 to B5 type. However, Cir X−1 has also exhibited type-I X-ray bursts (Tennant et al. 1986), which are characteristic of LMXBs. Furthermore, the fact that the companion star in Cir X−1 has yet to be decisively detected at optical wavelengths supports a possible LMXB nature for the system. Johnston et al. (2016) concluded that the optical counterpart in Cir X−1 could either be an unevolved low-mass star or a giant star that is still in the process of recovering from the supernova explosion that occurred less than 5000 yr ago. Due to the ambiguity surrounding the nature of Cir X−1, the source has been included in both our LMXB and HMXB catalogues.

As mentioned previously, several objects included in RK03 and Liu07 have been removed from our catalogue. Sometimes this was necessary because objects reported as independent in RK03 and Liu07 represented the same source (in either of the catalogues). This was mainly due to large positional uncertainties at the time of the catalogue compilation, or in some cases because the objects are extragalactic. In the case of the former, we include only the element from the pair in our LMXB list with the most used name, omitting the other, and summing up all known data. In the extragalactic origin scenario, the corresponding source is removed as we only consider Galactic LMXBs. Our initial source list was therefore modified as follows:

- The relatively bright source 2A 0521−720, which is more commonly referred to as LMC X−2, is located in the LMC (as the name suggests). As we consider only Galactic objects, we exclude it from our catalogue.
- The same is true for RX J0532.7−6926 (located in LMC), and so it is also not included in the current catalogue.
- Two sources AX J1745.6−2901 and 1A 1742−289 listed in Liu07 actually correspond to the same LMXB, and as the name ‘AX J1745.6−2901’ is more commonly used, we combine information regarding the two from Liu07 under this name.
- The second case of identical sources is 1E 1743.1−2852 and SAX J1747.0−2853, and so again we gave the most popular name to the object, SAX J1747.0−2853.

3.3. Summary of other differences with respect to the Liu07 and RK03 catalogues

In addition to the problematic cases described above, and the overall expansion of the sample, several other changes have been made compared to Liu07 and RK03:

- To standardise the reported X-ray fluxes, we revised the energy ranges used in the Liu07 study. Instead of using a single range of 2–10 keV, we now present ‘soft’ and ‘hard’ X-ray fluxes separately, each in well-defined energy ranges.
- In addition, X-ray fluxes (absorbed) in our table are represented in cgs units (erg s^{-1} cm^{-2}, instead of Jy reported in Liu07), which are more commonly used and meaningful for X-ray sources. We also now report both maximum and minimum flux values for each of the two energy bands instead of only reporting the maximum, as done in Liu07.
- To better reflect various phenomenological features reported in the literature, we increased the number of flags used to describe the properties of the sources. In comparison to Liu07, where 11 flags were used, we use 17.
- Our new version of the LMXB catalogue has additional (in comparison with Liu07) columns for hydrogen column density, near- and mid-IR data (from 2MASS, VVV, WISE, literature, etc.), BP-RP colour, optical *Gaia*/StarHorse/literature data, and distances.
- In addition, we include up to six finding charts (from mid-IR images to hard X-ray bands) for each object, instead of just a reference to a finding chart.
- Finally, our catalogue now includes 349 objects, which is a 71% increase from the 204 objects listed in Liu07 and RK03 combined.

4. Summary and conclusions

In this paper, we present a new LMXB catalogue, which provides an up-to-date census of known LMXBs in the Galaxy with a variety of corresponding multi-wavelength information extracted from current optical/IR surveys. In total, the catalogue contains 349 sources and has 62 columns. Descriptions of the columns are presented in Table B.1. The full version of the catalogue can be obtained through the VizieR database[36], and can also be found on a dedicated website[37]. We ask authors who use our catalogue in their research to refer to us by citing this article, as well as by referring to the website link in either the acknowledgements or a footnote.

We would like to emphasise here that the origin of some of the sources listed in the catalogue is not yet certain; some sources have only been tentatively classified as LMXBs due to the similarity of their X-ray properties to those of the systems identified, with no counterparts found in other bands. Along with this article, a new similar catalogue of HMXBs is being published (Neumann et al. 2023). We hope that both catalogues will be useful tools for future studies, which includes (but is not limited to) population studies of various types of X-ray-emitting objects (especially XRBs), searches for new XRBs in ongoing and upcoming surveys, classification of unidentified

[36] https://cdsarc.cds.unistra.fr/cgi-bin/qcat?J/A+A
[37] http://astro.uni-tuebingen.de/~xrbcat

X-ray sources, and as training data-sets for machine learning classification algorithms (Yang et al. 2021, 2022). In particular, our catalogue be relevant in the context of the ongoing analysis of eROSITA survey data, which is expected to substantially increase the number of known XRBs (Doroshenko et al. 2014). We therefore plan to update our catalogues to the best of our ability to keep the ever-increasing census of the Galactic LMXBs up to date and accessible to the community.

Acknowledgements. This research has made use of the SIMBAD data base and VizieR catalogue access tool operated at CDS, Strasbourg, France, and NASA's Astrophysics Data System (ADS). This research has made use of "Aladin sky atlas" developed at CDS, Strasbourg Observatory, France. This work has made use of data from the European Space Agency (ESA) mission *Gaia* (`https://www.cosmos.esa.int/gaia`), processed by the *Gaia* Data Processing and Analysis Consortium (DPAC, `https://www.cosmos.esa.int/web/gaia/dpac/consortium`). Funding for the DPAC has been provided by national institutions, in particular the institutions participating in the *Gaia* Multilateral Agreement. We acknowledge the public data from *XMM-Newton*, CXO, ROSAT, *Swift*, INTEGRAL, WISE, 2MASS and VISTA. AA thanks Deutsche Forschungsgemeinschaft (DFG) for support through the eRO-STEP research unit project 414059771 (DO 2307/2-1 and WI 1860/19-1).

References

Anders, F., Khalatyan, A., Chiappini, C., et al. 2019, A&A, 628, A94
Anders, F., Khalatyan, A., Queiroz, A. B. A., et al. 2022, A&A, 658, A91
Archibald, A. M., Stairs, I. H., Ransom, S. M., et al. 2009, Science, 324, 1411
Armas Padilla, M., Corral-Santana, J. M., Borghese, A., et al. 2023, A&A, submitted [arXiv:2305.07691]
Arnason, R. M., Papei, H., Barmby, P., Bahramian, A., & Gorski, M. D. 2021, MNRAS, 502, 5455
Baglio, M. C., Mainetti, D., D'Avanzo, P., et al. 2014, A&A, 572, A99
Bagnoli, T., in't Zand, J. J. M., D'Angelo, C. R., & Galloway, D. K. 2015, MNRAS, 449, 268
Bahramian, A., & Degenaar, N. 2023, in Handbook of X-ray and Gamma-ray Astrophysics, eds. C. Bambi, & A. Santangelo (Singapore: Springer Nature), 120
Bahramian, A., Strader, J., Chomiuk, L., et al. 2018, ApJ, 864, 28
Bailer-Jones, C. A. L., Rybizki, J., Fouesneau, M., Mantelet, G., & Andrae, R. 2018, AJ, 156, 58
Bailer-Jones, C. A. L., Rybizki, J., Fouesneau, M., Demleitner, M., & Andrae, R. 2021, AJ, 161, 147
Barthelmy, S. D. 2004, SPIE Conf. Ser., 5165, 175
Baumann, M., Boch, T., Pineau, F.-X., et al. 2022, in Astronomical Society of the Pacific Conference Series, 532, 7
Blay, P., Camero, A., Connell, P., et al. 2008, in The 7th INTEGRAL Workshop, 78
Bogdanov, S., & Halpern, J. P. 2015, ApJ, 803, L27
Boller, T., Freyberg, M. J., Trümper, J., et al. 2016, A&A, 588, A103
Bonnefoy, M., Chauvin, G., Dumas, C., et al. 2009, A&A, 506, 799
Britt, C. T., Strader, J., Chomiuk, L., et al. 2017, ApJ, 849, 21
Burrows, D. N., Hill, J. E., Nousek, J. A., et al. 2005, Space Sci. Rev., 120, 165
Butters, O. W., Barlow, E. J., Norton, A. J., & Mukai, K. 2007, A&A, 475, L29
Butters, O. W., Norton, A. J., Mukai, K., & Tomsick, J. A. 2011, A&A, 526, A77
Chaty, S., Rahoui, F., Foellmi, C., et al. 2008, A&A, 484, 783
Chelovekov, I. V., Grebenev, S. A., Mereminskiy, I. A., & Prosvetov, A. V. 2017, Astron. Lett., 43, 781
Chen, H.-L., Chen, X., Tauris, T. M., & Han, Z. 2013, ApJ, 775, 27
Chenevez, J., Alizai, K., Lepingwell, V. A., et al. 2018, ATel, 11272, 1
Christian, D. J., & Swank, J. H. 1997, ApJS, 109, 177
Clark, G. W. 2018, ApJ, 852, 121
Coleiro, A., Chaty, S., Zurita Heras, J. A., Rahoui, F., & Tomsick, J. A. 2013, A&A, 560, A108
Coti Zelati, F., Papitto, A., de Martino, D., et al. 2019, A&A, 622, A211
Coti Zelati, F., Hugo, B., Torres, D. F., et al. 2021, A&A, 655, A52
Court, J. M. C., Altamirano, D., Albayati, A. C., et al. 2018, MNRAS, 481, 2273
Cutri, R. M., Skrutskie, M. F., van Dyk, S., et al. 2003a, 2MASS All Sky Catalog of point sources (2MASS)
Cutri, R. M., Skrutskie, M. F., van Dyk, S., et al. 2003b, VizieR Online Data Catalog, II/246
Cutri, R. M., Wright, E. L., Conrow, T., et al. 2021, VizieR Online Data Catalog, II/328
Dalton, G. B., Caldwell, M., Ward, A. K., et al. 2006, SPIE Conf. Ser., 6269, 62690X
De Luca, A., Caraveo, P. A., Mereghetti, S., Tiengo, A., & Bignami, G. F. 2006, Science, 313, 814
Deutsch, E. W., Margon, B., & Anderson, S. F. 2000, ApJ, 530, L21
Doroshenko, V., Ducci, L., Santangelo, A., & Sasaki, M. 2014, A&A, 567, A7
Doroshenko, R., Santangelo, A., Doroshenko, V., Suleimanov, V., & Piraino, S. 2015, MNRAS, 452, 2490
Emerson, J., McPherson, A., & Sutherland, W. 2006, The Messenger, 126, 41
Engel, M. C., Heinke, C. O., Sivakoff, G. R., Elshamouty, K. G., & Edmonds, P. D. 2012, ApJ, 747, 119
Evans, I. N., Primini, F. A., Glotfelty, K. J., et al. 2010, ApJS, 189, 37
Evans, P. A., Page, K. L., Osborne, J. P., et al. 2020, ApJS, 247, 54
Fernique, P., Allen, M. G., Boch, T., et al. 2015, A&A, 578, A114
Foight, D. R., Güver, T., Özel, F., & Slane, P. O. 2016, ApJ, 826, 66
Fortin, F., Chaty, S., Coleiro, A., Tomsick, J. A., & Nitschelm, C. H. R. 2018, A&A, 618, A150
Fortin, F., García, F., Simaz Bunzel, A., & Chaty, S. 2023, A&A, 671, A149
Gaia Collaboration (Prusti, T., et al.) 2016, A&A, 595, A1
Gaia Collaboration (Brown, A. G. A., et al.) 2018, A&A, 616, A1
Gaia Collaboration (Brown, A. G. A., et al.) 2021, A&A, 649, A1
Gaia Collaboration (Vallenari, A., et al.) 2023, A&A, 674, A1
Galloway, D. K., Yao, Y., Marshall, H., Misanovic, Z., & Weinberg, N. 2010, ApJ, 724, 417
Gehrels, N., Chincarini, G., Giommi, P., et al. 2004, ApJ, 611, 1005
Giles, A. B., Swank, J. H., Jahoda, K., et al. 1996, ApJ, 469, L25
Gorgone, N., Kouveliotou, C., Younes, G., & Kennea, J. 2018, ATel, 11317, 1
Greiss, S., Steeghs, D., Maccarone, T., et al. 2011, ATel, 3688, 1
Grimm, H. J., Gilfanov, M., & Sunyaev, R. 2002, A&A, 391, 923
Heinke, C. O., Tomsick, J. A., Yusef-Zadeh, F., & Grindlay, J. E. 2009, ApJ, 701, 1627
Heinz, S., Sell, P., Fender, R. P., et al. 2013, ApJ, 779, 171
Jansen, F., Lumb, D., Altieri, B., et al. 2001, A&A, 365, L1
Jaodand, A. D., Deller, A. T., Gusinskaia, N., et al. 2021, ApJ, 923, 3
Johnston, H. M., Soria, R., & Gibson, J. 2016, MNRAS, 456, 347
Jonker, P. G., Fender, R. P., Hambly, N. C., & van der Klis, M. 2000, MNRAS, 315, L57
Jonker, P. G., Nelemans, G., & Bassa, C. G. 2007, MNRAS, 374, 999
Karasev, D. I., Lutovinov, A. A., & Burenin, R. A. 2008, Astron. Lett., 34, 753
Kaur, R., Wijnands, R., Patruno, A., et al. 2009, MNRAS, 394, 1597
Kaur, R., Heinke, C., Kotulla, R., et al. 2011, ATel, 3695, 1
Kennedy, M. R., Breton, R. P., Clark, C. J., et al. 2020, MNRAS, 494, 3912
Knight, A. H., Ingram, A., van den Eijnden, J., et al. 2023, MNRAS, 520, 3416
Krivonos, R., Tsygankov, S., Lutovinov, A., et al. 2012, A&A, 545, A27
Kuranov, A. G., & Postnov, K. A. 2015, Astron. Lett., 41, 114
Lamb, D. Q., Miller, M. C., & Taam, R. E. 1996, arXiv e-prints, [arXiv:astro-ph/9604089]
Lasota, J.-P. 2016, Black Hole Accretion Discs, 440 (Springer), 1
Li, K.-L., Strader, J., Miller-Jones, J. C. A., Heinke, C. O., & Chomiuk, L. 2020, ApJ, 895, 89
Liu, Q. Z., van Paradijs, J., & van den Heuvel, E. P. J. 2006, A&A, 455, 1165
Liu, Q. Z., van Paradijs, J., & van den Heuvel, E. P. J. 2007, A&A, 469, 807
Marocco, F., Eisenhardt, P. R. M., Fowler, J. W., et al. 2021, ApJS, 253, 8
Martí, J., Combi, J. A., Pérez-Ramírez, D., et al. 2007, A&A, 462, 1065
Masetti, N., Nucita, A. A., & Parisi, P. 2012, A&A, 544, A114
Matsuoka, M., Kawasaki, K., Ueno, S., et al. 2009, PASJ, 61, 999
Merloni, A., Predehl, P., Becker, W., et al. 2012, arXiv e-prints, [arXiv:1209.3114]
Middleditch, J., & Nelson, J. 1976, ApJ, 208, 567
Miller, J. M., Swihart, S. J., Strader, J., et al. 2020, ApJ, 904, 49
Minniti, D., Lucas, P. W., Emerson, J. P., et al. 2010, New A, 15, 433
Nespoli, E., Fabregat, J., & Mennickent, R. E. 2010, A&A, 516, A94
Neumann, M., Avakyan, A., Doroshenko, V., & Santangelo, A. 2023, A&A, submitted [arXiv:2303.16137]
Nucita, A. A., Carpano, S., & Guainazzi, M. 2007, A&A, 474, L1
Oh, K., Koss, M., Markwardt, C. B., et al. 2018, ApJS, 235, 4
Paduano, A., Bahramian, A., Miller-Jones, J. C. A., et al. 2021, MNRAS, 506, 4107
Papitto, A., Ferrigno, C., Bozzo, E., et al. 2013, Nature, 501, 517
Peng, S., & Shen, R.-F. 2021, ApJ, 916, 80
Predehl, P., Andritschke, R., Arefiev, V., et al. 2021, A&A, 647, A1
Rai, B., Pradhan, P., & Paul, B. C. 2018, Res. Astron. Astrophys., 18, 148
Ratti, E. M., Bassa, C. G., Torres, M. A. P., et al. 2010, MNRAS, 408, 1866
Ratti, E. M., van Grunsven, T. F. J., Torres, M. A. P., et al. 2013, MNRAS, 431, L10
Revnivtsev, M. G., Kniazev, A., Karasev, D. I., Berdnikov, L., & Barway, S. 2013, Astron. Lett., 39, 523
Ritter, H., & Kolb, U. 2003, A&A, 404, 301

Roberts, M. S. E. 2013, in Neutron Stars and Pulsars: Challenges and Opportunities after 80 years, 291, ed. J. van Leeuwen, 127
Rodriguez, J., Tomsick, J. A., & Chaty, S. 2008, A&A, 482, 731
Salvetti, D., Mignani, R. P., De Luca, A., et al. 2015, ApJ, 814, 88
Sato, T., Negoro, H., Iwakiri, W., et al. 2019, ATel, 13328, 1
Sazonov, S., Paizis, A., Bazzano, A., et al. 2020, New A Rev., 88, 101536
Schartel, N., González-Riestra, R., Kretschmar, P., et al. 2022, in Handbook of X-ray and Gamma-ray Astrophysics, eds. C. Bambi, & A. Santangelo (Singapore: Springer Nature), 114
Schlafly, E. F., Meisner, A. M., & Green, G. M. 2019, ApJS, 240, 30
Sguera, V., Bazzano, A., Bird, A. J., et al. 2006, ApJ, 646, 452
Shahbaz, T., Watson, C. A., Zurita, C., Villaver, E., & Hernandez-Peralta, H. 2008, PASP, 120, 848
Sidoli, L., Romano, P., Cucchiara, A., et al. 2007, ATel, 1089, 1
Skrutskie, M. F., Cutri, R. M., Stiening, R., et al. 2006, AJ, 131, 1163
Stelzer, B., Klutsch, A., Coffaro, M., Magaudda, E., & Salvato, M. 2022, A&A, 661, A44
Strader, J., Swihart, S. J., Urquhart, R., et al. 2021, ApJ, 917, 69
Sugizaki, M., Mitsuda, K., Kaneda, H., et al. 2001, ApJS, 134, 77
Swihart, S. J., Strader, J., Shishkovsky, L., et al. 2018, ApJ, 866, 83
Tananbaum, H., Gursky, H., Kellogg, E. M., et al. 1972, ApJ, 174, L143
Tendulkar, S. P., Kaspi, V. M., Archibald, R. F., & Scholz, P. 2017, ApJ, 841, 11
Tennant, A. F., Fabian, A. C., & Shafer, R. A. 1986, MNRAS, 221, 27P
Tetarenko, A., Sivakoff, G. R., Bahramian, A., et al. 2016, ATel, 8744, 1
Torres, M. A. P., Repetto, S., Wevers, T., et al. 2019, MNRAS, 487, 2296
Truemper, J. 1982, Adv. Space Res., 2, 241
Vincentelli, F. M., Cavecchi, Y., Casella, P., et al. 2020, MNRAS, 495, L37
Voges, W., Aschenbach, B., Boller, T., et al. 1999, A&A, 349, 389
Wachter, S., Wellhouse, J. W., Patel, S. K., et al. 2005, ApJ, 621, 393
Walter, R., Zurita Heras, J., Bassani, L., et al. 2006, A&A, 453, 133
Webb, N. A., Coriat, M., Traulsen, I., et al. 2020, A&A, 641, A136
Weisskopf, M. C., Tananbaum, H. D., Van Speybroeck, L. P., & O'Dell, S. L. 2000, SPIE Conf. Ser., 4012, 2
Winkler, C., Pace, O., & Volonté, S. 1993, ESA J., 17, 207
Winkler, C., Courvoisier, T. J. L., Di Cocco, G., et al. 2003, A&A, 411, L1
Wright, E. L., Eisenhardt, P. R. M., Mainzer, A. K., et al. 2010, AJ, 140, 1868
Yang, H., Hare, J., Volkov, I., & Kargaltsev, O. 2021, RNAAS, 5, 102
Yang, H., Hare, J., Kargaltsev, O., et al. 2022, ApJ, 941, 104

Appendix A: Optical/IR counterparts

Table A.1. Identified archive optical/IR counterparts of LMXBs.

Source name	*Gaia* DR3	*2MASS*	*CatWISE*2020
	Based on optical/IR/radio follow-ups:		
MAXI J0556−332	2890346074897001216		
4FGL J0427.8−6704	4656677385699742208	J04274958−6704350	J042749.64−670435.0
IGR J17494−3030	4056028099172996352		
1FGL J1417.7-4407	6096705840454620800	J14173057−4402574	J141730.57−440257.5
XTE J1637−498	5940421734427982336	J16370267−4951401	
MAXI J1807+132	4497207964419829632		
3A 1837+049	4283919201304278912	J18395759+0502113	J183957.57+050210.5
MAXI J1828−249	4076998775244833280		
1RXS J180408.9−342058	4042163562572848384		
IGR J17091-3624	5976921951382731520		J170907.75−362425.0
IGR J17585−3057	4044163406621956992		J175829.80−305702.3
4U 1543−624	5826501373348972288		
Swift J1858.6−0814	4203799300867262720		
MAXI J1305−704	5843823766718594560		J130655.74−702704.2
IGR J17329−2731	4061336747511224704	J17325067−2730015	J173250.54−273003.4
IGR J16358−4726		J16355369−4725398	J163553.75−472541.0
XMMU J174445.5−295044		J17444541−2950446	J174445.43−295044.5
IGR J17454−2919		J17452768−2919534	
4U 1705−250	4112450294268643456		
4FGL J0540.0−7552	4648562676357022208		J054001.80−755419.7
3FGL J1544.6−1125	6268529198286308224		J154439.38−112804.5
CXOU J110926.4−650224	5240167590731178624		J110926.21−650227.1
4FGL J0407.7−5702	4682464743003293312		J040731.65−570025.1
1RXH J173523.7−354013	5974787971132982144		
IGR J16287−5021	5934583950467938304		
4U 1556−60	5833042299288099072		
EXO 1846−031	4258794192383316864	J18491710−0303559	J184917.08−030355.3
AX J1735.8−3207	4055019091071763712	J17354627−3207099	
IGR J16293−4603	5942210433690960640	J16291285−4602506	J162912.85−460250.4
4U 1626−67	5809528276749789312		
SAX J1810.8−2609	4064636102946481408		
XTE J1709−267	4108865783346597760		
XTE J1710−281	4108449755564592256		
IGR J19308+0530	4294249387962232576	J19305075+0530582	J193050.75+053058.0
Swift J2037.2+4151		J20370560+4150051	J203705.60+415005.2
GS 1826−238	4077372536242802944		
SRGA J181414.6−225604	4066460746608630912	J18141475−2256195	J181414.78−225619.4

Table A.1. continued

Source name	*Gaia* DR3	*2MASS*	*CatWISE*2020
	Based on Arnason et al. (2021):		
GRO J1655−40	5969790961312131456	J16540014−3950447	J165400.13−395044.7
SWIFT J061223.0+701243	1107229825742589696		J061222.63+701243.1
1A 1246−588	6059778089610749440		J124939.17−590516.3
MXB 1659−29	6029391608332996224		
SAX J1711.6−3808	5973177495780065664	J17113714−3807073	J171137.14−380707.4
4U 1724−307	4058208396397618688	J17273315−3048076	J172733.28−304809.0
EXO 1747−214	4118590585673834624		
4U 1755−33	4042473487415175168		
HETE J1900.1−2455	4074363039644919936		
4U 1915−05	4211396994895217152		
XTE J1901+014	4268294763113217152		

Appendix B: Catalogue format

Table B.1. Description of columns in the LMXB catalogue table.

№	Column name	Unit	Description
1	'Name'		Object name, which is the most common name in the literature.
2	'RAdeg'	deg	Right Ascension in degrees (ICRS).
3	'DEdeg'	deg	Declination in degrees (ICRS).
4	'PosErr'	arcsec	Positional error in arcseconds.
5	'Coord_Ref'		The source from which the position of the object is taken.
6	'GLON'	deg	Galactic longitude in degrees.
7	'GLAT'	deg	Galactic latitude in degrees.
8	'Xray_Type'		List of the X-ray types assigned to the object. For more information see Sect. 2.1.
9	'Porb'	day	Orbital period of the binary system in days.
10	'Ppulse'	s	Pulsation period (spin) of a NS in seconds.
11	'Alt_Name'		Most frequently used alternative name.
12	'SpType'		Spectral type of the optical counterpart.
13	'Vmag'	mag	Optical magnitude in V-band according to SIMBAD database and literature.
14	'e_Vmag'	mag	Corresponding magnitude error in V-band.
15	'Gaia_DR3_ID'		Name in Gaia DR3(eDR3) catalogue.
16	'Gmag'	mag	Optical magnitude in G-band according to a Gaia catalogue or the literature.
17	'e_Gmag'	mag	Corresponding magnitude error in G-band.
18	'BP-RP'	mag	BP-RP colour.
19	'2MASS_ID'		Name in 2MASS catalogue.
20	'Jmag'	mag	IR magnitude in J-band according to 2MASS or the literature.
21	'e_Jmag'	mag	Corresponding magnitude error in J-band according to 2MASS or the literature.
22	'Hmag'	mag	IR magnitude in H-band according to 2MASS or the literature.
23	'e_Hmag'	mag	Corresponding magnitude error in H-band according to 2MASS or the literature.
24	'Kmag'	mag	IR magnitude in K-band according to 2MASS or literature.
25	'e_Kmag'	mag	Corresponding magnitude error in K-band according to 2MASS or the literature.
26	'WISE_ID'		Name in CatWISE, AllWISE, or WISE catalogue.
27	'W1mag'	mag	IR magnitude in W1 WISE band.
28	'e_W1mag'	mag	Corresponding magnitude error in W1 WISE band.
29	'W2mag'	mag	IR magnitude in W2 WISE band.
30	'e_W2mag'	mag	Corresponding magnitude error in W2 WISE band.
31	'N_H'	10^{22}cm^{-2}	Neutral hydrogen column density.
32	'MinSoftFlux'	10^{-12}erg/s/cm^2	Minimum flux (absorbed) from a source in soft X-ray.
33	'MaxSoftFlux'	10^{-12}erg/s/cm^2	Maximum flux (absorbed) from a source in soft X-ray.
34	'Soft_Xray_Var		Ratio of maximal soft X-ray flux and minimal soft X-ray flux.
35	'Soft_Xray_Range'	keV	Soft X-ray flux energy range used.
36	'MinHardFlux'	10^{-12}erg/s/cm^2	Minimum flux (absorbed) from a source in hard X-ray.
37	'MaxHardFlux'	10^{-12}erg/s/cm^2	Maximum flux (absorbed) from a source in hard X-ray.
38	'Hard_Xray_Var'		Ratio of maximal hard X-ray flux and minimal hard X-ray flux.
39	'Hard_Xray_Range'	keV	Hard X-ray flux energy range used.
40	'AG'	mag	G-band absorption A_G.
41	'Mean_Dist'	pc	Mean estimate of the distance to the binary system.

Table B.1. continued

№	Column name	Unit	Description
42	'Low_Dist'	pc	The lowest (minimum) estimate of the distance to the binary system.
43	'High_Dist'	pc	The highest (maximum) estimate of the distance to the binary system.
44	'Incl'	deg	Binary system inclination.
45	'Mx'	$M_\odot$	Mass of the compact object.
46	'Mopt'	$M_\odot$	Mass of the optical counterpart.
47	'B-V'	mag	B-V colour index.
48	'E(B-V)'	mag	E(B-V) colour excess.
49	'tMSP_Flag'		tMSP flag, which can take one of the two values, indicating that the source is:
			1 – one of the three solidly considered tMSPs.
			2 – a tMSP candidate.
50	'Liu07_IDX'		Ordinal number of the source in the table of Liu07 LMXB catalogue.
51	'RK03_IDX'		Ordinal number of the source in the table of RK03 LMXB catalogue.
52	'Orb_Ref'		Orbital period origin reference.
53	'Pulse_Ref'		Spin (pulsation) period of the NS origin reference.
54	'Spect_Ref'		Reference to the origin of the optical spectral type of the star.
55	'Vmag_Ref'		Reference to the origin of the V-band magnitude.
56	'Gmag_Ref'		Reference to the origin of the G-band magnitude.
57	'JHK_Ref'		Reference to the origin of the JHK information.
58	'WISE_Ref'		Reference to the WISE IR catalogue used (CatWISE, AllWISE or WISE).
59	'N_H_Ref'		N_H value origin reference.
60	'AG_Ref'		Reference to the origin of the G-band absorption A_G .
61	'Dist_Ref'		Reference to the origin of the distance estimations.
62	'Mass_Ref'		Reference to the origin of the mass estimations.